

Supplemental: Inverse Design Framework with Invertible Neural Networks for Passive Vibration Suppression in Phononic Structures

1 Derivation of the Transfer Matrix Method (TMM) For Euler-Bernoulli Beam

The transverse structural dynamics of an Euler-Bernoulli beam is given by:

$$EI \frac{\partial^4}{\partial x^4} w(x, t) + \rho A \frac{\partial^2}{\partial x^2} w(x, t) = 0 \quad (1)$$

$$w(x, t) = \bar{W}(x) e^{i\omega t}$$

where E is the elastic modulus, I is the moment of inertia, ρ is the material density, and A is the cross-sectional area. Through separation of variables, the transverse displacement of the beam $w(x, t)$ can be expressed using a spatial function $\bar{W}(x)$ and a time-harmonic term with ω being the angular frequency (expressed in rad/s). As such, Eq. [1] can be rewritten as :

$$\left(EI \frac{\partial^4}{\partial x^4} - \rho A \omega^2 \right) \bar{W}(x) e^{i\omega t} = 0 \quad (2)$$

Considering $\bar{W}(x) = \beta e^{i\kappa x}$ where κ denotes the angular wavenumber (i.e., spatial frequency), we get:

$$\kappa = \pm \omega \sqrt{\frac{\rho A}{EI}} \quad (3)$$

and

$$\bar{W}(x) = \sum_{i=1}^4 \beta_i e^{i\kappa_i x} \quad (4)$$

$$\bar{\kappa} = \sqrt[4]{\frac{\omega^2 \rho A}{EI}}, \quad \kappa_1 = \bar{\kappa}, \quad \kappa_2 = i\bar{\kappa}, \quad \kappa_3 = -\bar{\kappa}, \quad \kappa_4 = -i\bar{\kappa}$$

The TMM equations follow four states of the beam which comprise two elastic deformations: the beam's transverse displacement $\bar{W}(x)$ and bending angle $\bar{\phi}(x)$; and two forcing

functions: the beam's bending moment $\bar{M}(x)$ and shear force $\bar{V}(x)$. We define a state vector Ψ such that:

$$\Psi = \begin{bmatrix} \bar{W}(x) \\ \bar{\phi}(x) \\ \bar{M}(x) \\ \bar{V}(x) \end{bmatrix} = \begin{bmatrix} \bar{W} \\ \frac{d\bar{W}}{dx} \\ -EI \frac{d^2\bar{W}}{dx^2} \\ -EI \frac{d^3\bar{W}}{dx^3} \end{bmatrix} \quad (5)$$

Finally, substituting Eq.[3] in 5, we get:

$$\Psi_R = HDH^{-1}\Psi_L$$

$$H = \begin{bmatrix} 1 & 1 & 1 & 1 \\ \kappa_2 & \kappa_3 & \kappa_4 & \kappa_1 \\ -EI(\kappa_2)^2 & -EI(\kappa_3)^2 & -EI(\kappa_4)^2 & -EI(\kappa_1)^2 \\ -EI(\kappa_2)^3 & -EI(\kappa_3)^3 & -EI(\kappa_4)^3 & -EI(\kappa_1)^3 \end{bmatrix} \quad (6)$$

$$D = \begin{bmatrix} e^{\kappa_2 d} & 0 & 0 & 0 \\ 0 & e^{\kappa_3 d} & 0 & 0 \\ 0 & 0 & e^{\kappa_4 d} & 0 \\ 0 & 0 & 0 & e^{\kappa_1 d} \end{bmatrix}$$

where $\bar{T} = HDH^{-1}$ is the transfer matrix.

The frequency-dependent transmissibility ratio $T_R(\omega)$ is then given by:

$$T_R(\omega) = \frac{\bar{W}(x_L)}{\bar{V}(x_R)}$$

$$T_R(\omega) = (A \times E) - (B \times E) - C + D$$

$$A = \bar{T}[1, 1]$$

$$B = \frac{\bar{T}[1, 2] \times \bar{T}[4, 1]}{\bar{T}[4, 2]}$$

$$C = \frac{\bar{T}[1, 2] \times \bar{T}[4, 4]}{\bar{T}[4, 2]} \quad (7)$$

$$D = \bar{T}[1, 4]$$

$$E = \frac{(\bar{T}[3, 2] \times \bar{T}[4, 4]) - (\bar{T}[3, 4] \times \bar{T}[4, 2])}{(\bar{T}[3, 1] \times \bar{T}[4, 2]) - (\bar{T}[3, 2] \times \bar{T}[4, 1])}$$

Table 1: Optimization results generated using INN-based initial (inverse) design, where the INN is fed with the artificial transmissibility ratio vector

Non-Resonant Freq. Range (NRFR) Query	# Trials	Periodic: Final Solution		Aperiodic: Final Solution	
		Constraint Violation	Mass (Kg)	Constraint Violation	Mass (Kg)
4000-5500Hz	1	0	697.28	3 (Infeasible)	425.76

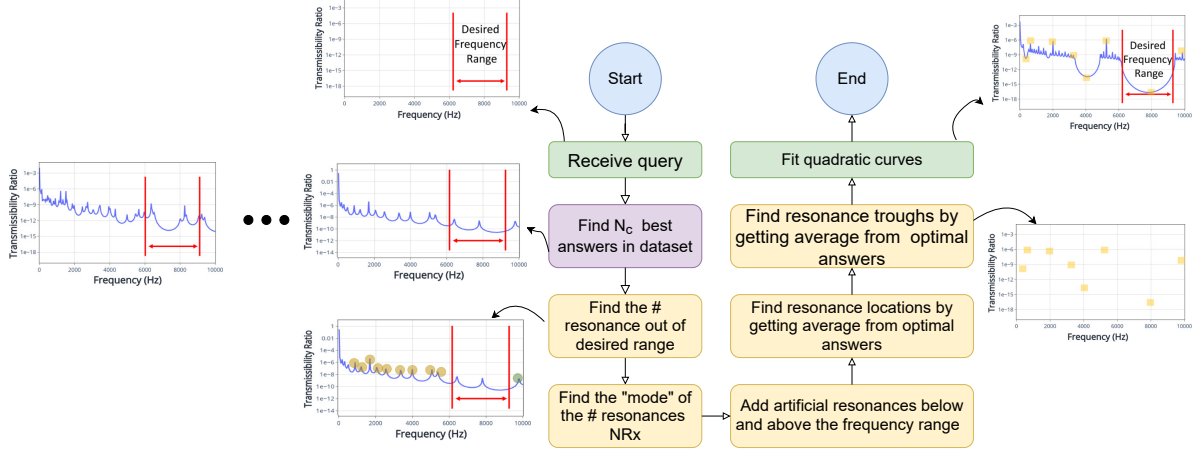


Fig. 1: Procedure to translate a non-resonant frequency range query $([\omega_L, \omega_U])$ to a complete output vector of Transmissibility Ratios $([T_{R1}, T_{R2}, \dots, T_{R80}])$ that can be fed to the INN; the INN is then executed in reverse to retrieve the corresponding input design

where x_L and x_R signify the left and right ends of the beam, respectively, and $\bar{T}[i, j]$ equals the value present in the i^{th} row and j^{th} column of the transfer matrix \bar{T} .

2 Translating Query to Target Response

Procedure for Translating NRFR Query to Transmissibility Ratios: While the user's query defines the non-resonant frequency range (NRFR), $[\omega_L, \omega_U]$, the INN requires the entire vector T_R of transmissibility ratios to work. Our earlier-stated approach of setting all peaks to a $T_R = 0.01$ helps; however, we are still left with no knowledge of the T_R values beyond the $[\omega_L, \omega_U]$ range. To be able to generalize the inverse retrieval process, we therefore developed a preliminary procedure to translate the NRFR query to an artificial T_R vector, as shown in Fig. 1.

In this procedure, first we choose N_C responses with the highest feasibility over training samples. Then the resonance frequencies beyond the NRFR, i.e., for $\omega \leq \omega_L$ and $\omega \geq \omega_U$, are calculated. The number of resonances below and above the desired non-resonant frequency range is chosen based on the most common (mode) number of resonant peaks in the N_C samples $(N_{C,L}, N_{C,U})$. The average location of their resonance frequency is used to develop expected resonances. The troughs between two consecutive resonances are defined

based on the average location of the troughs in N_C samples. Finally, in order to find the T_R vector, quadratic functions are fitted to every successive resonant peaks and the troughs between them. This procedure creates an artificial T_R vector, which can then be used by INN (fed on the output end) for inversely predicting the design.

To explore the usability of this procedure, it was applied to create the initial design for the optimization of the periodic and aperiodic structures in the 4.0-5.5 kHz NRFR case. From Table 1 it can be seen that, while seeding INN with this artificially generated T_R vector leads to an ensuing optimized designs that are worse than those obtained when the INN is seeded directly with actual T_R vector, they are still better than the best-of-10 randomly initialized optimizations by having fewer or no resonance peaks in the given NRFR.